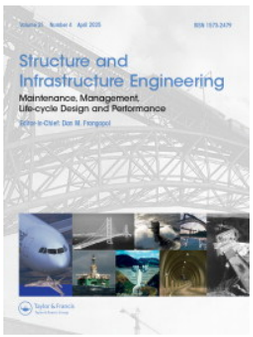

Taylor & Francis
Taylor & Francis Group

Structure and Infrastructure Engineering
Maintenance, Management, Life-Cycle Design and Performance

ISSN: (Print) (Online) Journal homepage: www.tandfonline.com/journals/nsie20

Reliability-based determination of allowable corrosion degree to define the end of lifetime of concrete elements in bending

Karel Van Den Hende, Wouter Botte, Stijn Matthys, Geert Lombaert & Robby Caspeele

To cite this article: Karel Van Den Hende, Wouter Botte, Stijn Matthys, Geert Lombaert & Robby Caspeele (06 Apr 2025): Reliability-based determination of allowable corrosion degree to define the end of lifetime of concrete elements in bending, Structure and Infrastructure Engineering, DOI: 10.1080/15732479.2025.2483503

To link to this article: https://doi.org/10.1080/15732479.2025.2483503

STRUCTURE AND INFRASTRUCTURE ENGINEERING
https://doi.org/10.1080/15732479.2025.2483503

Reliability-based determination of allowable corrosion degree to define the end of lifetime of concrete elements in bending

Karel Van Den Hende[a], Wouter Botte[a], Stijn Matthys[a], Geert Lombaert[b] and Robby Caspeele[a]

[a]Department of Structural Engineering and Building Materials, Ghent University, Ghent, Belgium; [b]Structural Mechanics, Civil Engineering Department, KU Leuven, Leuven, Belgium

ABSTRACT

The assessment of reinforcement corrosion of a concrete structure is challenging due to all the uncertainties regarding the corrosion process itself and subsequent effects on the structural capacity. In this work, a proxy criterium for the determination of a structural capacity-based end of lifetime is proposed, expressed as the allowable corrosion degree. This value can be compared with the predicted corrosion degree over time to detect the time instant where structural interventions are needed. The criterium is based on the allowable level of corrosion by lowering the target reliability level for a structure from the design to the assessment phase. The advantage of this criterium is that it can be used to have a prior assessment of the need for a maintenance strategy in absence of more detailed investigations by either predicting the corrosion degree over time or by determining the corrosion degree *in situ*. It is shown that the critical corrosion degree mainly depends on the type of variable loading and the load ratio describing the ratio of variable over total loading. Moreover, the critical corrosion degree is significantly lower for structures subjected to traffic loads compared to other load cases such as wind, snow or other imposed loads.

ARTICLE HISTORY
Received 2 September 2024
Revised 16 November 2024
Accepted 26 November 2024

KEYWORDS
Carbonation-induced corrosion; chloride-induced corrosion; end of lifetime; existing structures; structural reliability

1. Introduction

The assessment of existing structures is nowadays of tremendous importance due to the challenges in the management of an aging patrimony faced by decision-makers. For corroding reinforced concrete structures, an important evaluation parameter is the probability of depassivation, that marks the potential (depending on the presence of humidity and oxygen) start of the corrosion process. However, such criterion does not take into consideration the propagation phase and it does not allow to identify the point in time where corrosion has an adverse effect on the structural safety. Therefore, more work is needed to relate quantities associated with durability to the structural reliability of a structure (Alexander & Beushausen, 2019; Siemens et al., 1998).

In order to assess the structural reliability in an indirect way, a proxy criterium is proposed in this work. The criterium provides a limit for the expected corrosion degree of a reinforced concrete structure, which can be used in a straight-forward way by a decision-maker to determine which structures are more critical. Based on information (e.g. due to measurements) of the corrosion degree, the structure is evaluated by comparing the actual corrosion degree with the critical limit, which is derived in this work. If the critical corrosion degree is exceeded, a more in-depth assessment using an advanced limit state evaluation can be executed. This involves a more detailed evaluation of the governing parameters, such as concrete cover, concrete strength, etc. and an investigation of the actual loading situation.

This corrosion criterium is determined based on the target safety level, below which structural intervention becomes necessary (Allen, 1991; Caspeele et al., 2016; Diamantidis & Bazzurro, 2014; Markova et al., 2017; Schueremans & Van Gemert, 2004; Steenbergen et al., 2015; Steenbergen & Vrouwenvelder, 2010; Sykora et al., 2017; Vrouwenvelder et al., 2011; Vrouwenvelder & Scholten, 2010). There exists a common consensus that increasing the safety level of an existing structure will lead to higher costs when compared to an equivalent action in the design phase, which leads to a lower required target safety level for an existing structure compared to a new structure. In (Caspeele et al., 2016), it was proposed to reduce the safety level expressed as target reliability value $\beta_{t,50y}$, corresponding to a structure in the design phase and a reference period of 50 years, with a value of 0.5. However, for deteriorating structures, a reference period of 1 year was found to be more appropriate (Meinen & Steenbergen, 2018) and the target values $\beta_{t,1y}$ defined in Table 1 can be applied, shifting in the relative cost of safety measure to distinguish between the design and assessment of a structure. The derived target values are related to the optimal design situation in economic aspects, and are typically governing when compared to the criteria for human safety.

CONTACT Karel Van Den Hende karel.vandenhende@ugent.be Department of Structural Engineering and Building Materials, Ghent University, Technologiepark-Zwijnaarde 60, 9052 Ghent, Belgium

Table 1. Annual target reliability indices $\beta_{t,1y}$ for ultimate limit state of a structure ((ISO 2394, 2015) and (JCSS, 2000)).

	Consequence class (CC)		
Relative cost of safety measure	CC1	CC2	CC3
Large (A)	3.1	3.3	3.7
Normal (B)	3.7	4.2	4.4
Small (C)	4.2	4.4	4.7

The target safety level decreases when switching from the design phase to the assessment phase of a structure. As a result, less reinforcement is required to reach the (lower) target reliability for the assessment phase compared to the design phase. This can be considered as spare capacity in the resistance of the structure (assuming the load and structural behavior does not change), before the structure is considered to be unsafe. As a result, for a corroding structure, a critical corrosion degree can be defined, restricting the allowable loss of reinforcement area. This approach assumes that the initial reinforcement design corresponds to the target reliability for design, and that the original and present loading situation is the same, which is not always satisfied. Nevertheless, the results derived are generally applicable and independent of case-specific differences. As a result, this work provides insight into how much corrosion is allowed for a specific type of structure and can be very valuable when assessing a large patrimony of structures.

To assess the evolution in time of the reliability index, it is necessary to consider both the initiation phase (e.g. onset of corrosion) and the propagation phase (e.g. reduction of reinforcement area), combined with a limit state evaluation (Aslani & Dehestani, 2020; Bagheri et al., 2020; Nogueira et al., 2023; Nogueira & Leonel, 2013; Val & Melchers, 1997). However, quantifying the safety level over time can be cumbersome as the ultimate limit state needs to be evaluated at each time step in the future. In this work, the explicit evaluation of the ultimate limit state is replaced by defining a critical threshold for the percentage of reinforcement lost for a general case of a singly reinforced (only reinforcement at bottom) concrete beam with rectangular cross section that is subjected to bending. This leads to a much more efficient and practical evaluation by eliminating the need to explicitly predict the safety level over time.

The novelty of this work is expressed in the combination of adjusted target reliability values, durability models and resistance models, which have not been combined before to quantify the allowable corrosion loss for a general concrete structure. In the first part of this work, the critical threshold for the corrosion degree is proposed for a reinforced concrete beam subjected to bending, where the corrosion degree is considered either deterministic or stochastic. The results can be used to assess an existing structure, but can also be used to predict the service life in the design phase of a structure. Therefore, in the second part of this work, the loss of reinforcement steel area is predicted over time by predicting the corrosion degree for chloride-and carbonation-induced corrosion for a range of different exposure situations and designs, which can be compared with the threshold derived in the first part. Finally, the results are discussed and conclusions are proposed.

2. Critical corrosion degree based on annual target values

When assessing existing structures, it is considered more appropriate to adopt a lower $\beta_{t,1y}$-value compared to design, as generally the cost of a safety measure is higher than in the design phase. As a result, some spare capacity is present in the reinforcement area before corrosion leads to a critical situation where interventions are needed. It must be noted that it is here assumed that the reliability of the structure only decreases due to the effect of corrosion. In reality, the reliability level might further reduce due to other deterioration phenomena. On the other hand, the reliability level of a structure can also be considered to increase over time due to its proven performance, a beneficial effect not considered herein. The critical reinforcement loss is determined for a reinforced concrete beam subjected to bending, where the remaining reinforcement area is first considered deterministic, and afterwards considered uncertain according to a particular probability distribution.

2.1. Quantification of allowable corrosion degree as deterministic property

Consider a reinforced concrete beam with rectangular cross section, subjected to bending, as in the example used to validate the adjusted partial factors for fib MC2020 (Caspeele & Van Den Hende, 2023). The beam is subjected to a combination of a permanent (either self-weight or imposed) and a variable vertical load from either imposed loading, wind, traffic or snow. The limit state equation $Z(\boldsymbol{X})$ is given as follows:

$$Z(\boldsymbol{X}) = \theta_R R(A_s) - \theta_E[G + C_0 Q(\chi)] \quad (1)$$

Where $R(A_s)$ is the bending moment resistance corresponding to reinforcement area A_s, and the other parameters are listed in Tables 2–4. In Table 2, the characteristic values X_k are varied between certain bounds in order to consider different rectangular cross-sections designed according to EN 1992-1-1 (2004), as will be elaborated below.

The bending moment resistance of the beam R is determined by a cross-sectional analysis of the beam as illustrated in Figure 1, considering the hypothesis of Bernoulli is satisfied

Table 2. Range of design parameters and their probabilistic models (fib Model Code 2020, 2024).

Variable	Distribution	μ_X/X_k	$X_{k,\min}$	$X_{k,\max}$	V_X
Beam width $b[mm]$	Deterministic	1.0	200	600	/
Beam height $h[mm]$	Deterministic	1.0	400	800	/
Concrete cover $X[mm]$	Gamma	1.0	20	40	0.17
Steel strength $f_y[MPa]$	Lognormal	1.07	400	500	0.045
Concrete strength $f_c[MPa]$	Lognormal	1.19	20	40	0.10
Permanent load $G[kNm]$	Normal	1.0	30	60	0.04 or 0.10[a]
Load ratio $\chi = \frac{Q_k}{G_k+Q_k}$ [-]	Deterministic	1.0	0.1	0.7	/

[a]0.04 for self-weight; 0.1 for imposed load.

(cross-section remains straight during bending). The stress-strain diagrams used for the concrete in compression (parabolic-rectangular) and reinforcement steel in tension (bilinear) are shown in Figure 2. For the reinforcement, the material is assumed to be in the yielding stage at the ultimate limit state and the ultimate strain ε_u is fixed at 1.0%. In case of corrosion, the ultimate strain for steel decreases as the steel becomes more brittle, which can be quantified by (Yu et al., 2015):

$$\frac{\varepsilon_{u,corr}}{\varepsilon_u} = \begin{cases} e^{-\alpha/10} & for\ \alpha \leq 15\% \\ 0.2 & for\ \alpha > 15\% \end{cases} \quad (2)$$

Where α is the corrosion degree, expressed as the ratio of the lost reinforcement area over the original value $A_{s,0}$ (in %). Typically, also the steel strength decreases due to corrosion which is not considered in this work as it is generally less pronounced than the loss of area and ultimate strain. Moreover, the loss of steel strength is compensated by the fact that the stress-strain diagram of steel makes use of a horizontal plateau at the level of the yielding strength, and thus the full strength is not exploited in the first place. The stress-strain relationship of concrete is described by:

$$\sigma_c = \begin{cases} f_c\left[1-\left(1-\frac{\varepsilon_c}{\varepsilon^*_{c2}}\right)^2\right] & for \quad \varepsilon_c \leq \varepsilon^*_{c2} \\ f_c & for \quad \varepsilon^*_{c2} < \varepsilon_c \leq \varepsilon^*_{cu2} \end{cases} \quad (3)$$

And the strain limits ε^*_{c2} and ε^*_{cu2} are fixed at 0.20% and 0.35%, respectively. The properties of concrete are considered to be unaffected by corrosion.

An important parameter to consider is the model uncertainty for the flexural capacity of a corroded reinforced concrete beam θ_R. In literature, the error of the prediction model for the flexural capacity has been investigated by Azad et al. (2010) and Azher (2005), among others. However, to the knowledge of the authors, no consensus has been reached regarding which model uncertainty is most suited for the current application. Moreover, in order to have a compatible approach, the model uncertainty of a corroded beam should converge to the model uncertainty for an uncorroded beam if the corrosion degree approaches zero. As such a model uncertainty is not developed yet (to the knowledge of the authors), it is chosen to maintain the same model uncertainty for the original and corroded beams.

Table 3. Probabilistic models for variables independent of design or loads (fib Model Code 2020, 2024).

Variable	Distribution	μ_X	V_X
Resistance model uncertainty $\theta_R[-]$	Lognormal	1.09	0.045
Load effect model uncertainty $\theta_E[-]$	Lognormal	1.0	0.075
Conversion factor in-situ cast concrete $\eta[-]$	Lognormal	0.95	0.12

Considering a set of input parameters (load types, load ratio χ and characteristic values b_k, h_k, a_k, f_{yk}, f_{ck} and G_k), a range of First Order Reliability Method (FORM) analyses are performed in order to find the reinforcement areas $A_{s,0}$ and $A_{s,crit}$ that correspond to the annual target reliability values $\beta_{t,1y}$ for respectively, the design (normal cost type B) and assessment (high cost type A) of structures defined in Table 1. The corrosion degree determines both the remaining steel area, while it also reduces the ultimate strain of the steel following Equation (2). This results in the allowable (critical) corrosion degree $\alpha_{crit} = \frac{A_{s,0}-A_{s,crit}}{A_{s,0}}$ or the critical reinforcement area for each specific set of input parameters.

The procedure is illustrated in Figure 3 and starts from a fixed consequence class (CC), permanent and variable load type, and load ratio χ, but varying the other input parameters (b_k, h_k, X_k, f_{yk}, f_{ck}, G_k) by taking Latin Hypercube Samples (LHS) (Olsson et al., 2003) randomly within their range defined in Table 2. In total, 100 samples are generated, which was iteratively found to converge to a fixed result. Afterwards, the calculation is repeated for different values of CC, permanent and variable load types and the range of results of the critical corrosion degree α are shown in Figures 4 (for CC1), Figure 5 (for CC2) and Figure 6 (for CC3).

The results are very similar for $V_G = 0.04$ and $V_G = 0.10$, which shows that the type of permanent load does not significantly affect the critical corrosion degree. The influence of the consequence class (CC) is not linear as the critical corrosion degree is largest for CC2. This shows that the relative difference, expressed in terms of corrosion degree, between the reliability levels of CC2 is larger compared to the other consequence classes. Thirdly, the range of results is narrow, which shows that also the influence of the design parameters (listed in Table 2) on the allowable corrosion degree is relatively small. This makes the proposed values for the reliability-based allowable corrosion degrees rather case-independent and hence robust. However, the load ratio χ and type of variable loading have a substantial effect on the critical corrosion degree. An increase in the load ratio χ means that the amount of variable load (with respect to permanent load) increases. As the variable load is typically associated with more uncertainty, the entire load effect becomes more variable. As a result, the applied load has a larger influence on the reliability index and an increase of the corrosion level affects the reliability index to a smaller extent. As a result, the critical corrosion degree α_{crit} increases with the load ratio χ.

Traffic loads are associated with less uncertainty, thus in general the uncertainty on the load effect has a lower influence on the reliability index, which explains the difference

Table 4. Probabilistic models for variable loads for a reference period of 1 year (fib Model Code 2020, 2024).

Variable	Type	Distribution	μ_X/X_k	V_X
Time-variant component variable load Q	Imposed load	Gumbel	0.20	1.1
	Wind load	Gumbel	0.60	0.32
	Traffic load	Gumbel	0.73	0.075
	Snow load	Gumbel	0.37	0.65
Time-invariant component variable load C_0	Imposed load	Lognormal	1.0	0.10
	Wind load	Lognormal	0.65	0.30
	Traffic load	Lognormal	1.0	0.10
	Snow load	Lognormal	0.80	0.20

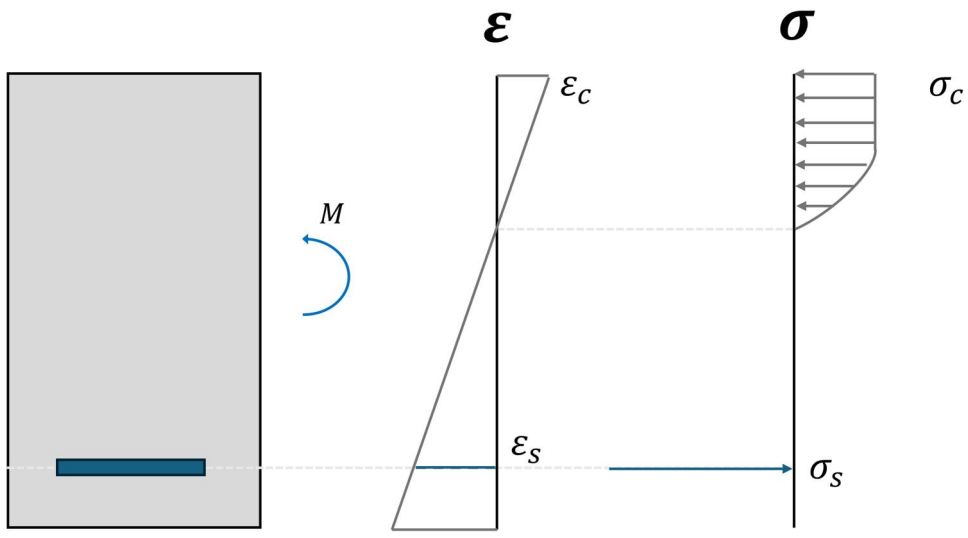

Figure 1. Strain and stress diagram to calculate moment capacity in ultimate limit state.

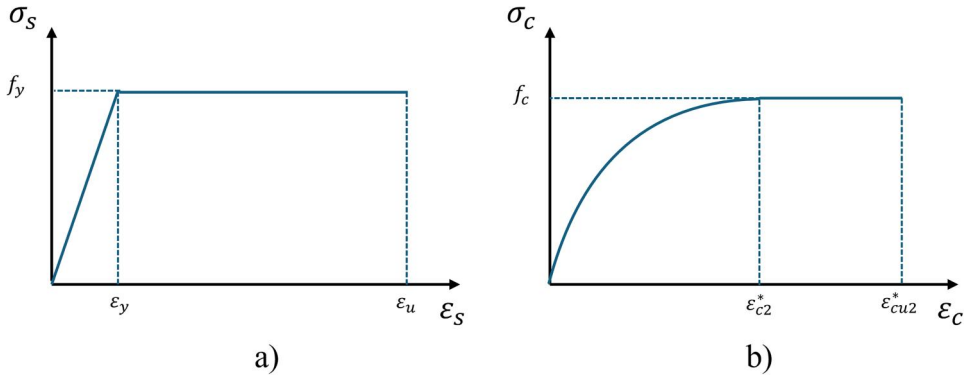

Figure 2. Constitutive law for a) reinforcement steel and b) concrete.

in results between the traffic load and the other types of variable load. However, this causes structures subjected to traffic loads, such as road bridges, to be more prone to corrosion. Additionally, these bridges are commonly subjected to chlorides due to deicing salts and traffic loads tend to increase over time which makes the structures even more critical. Between the other types of variable loading (imposed, wind and snow) there is no significant difference in the corrosion degree. The uncertainty related to these loading types is close to each other, and therefore their sensitivity on the reliability index is similar. As a result, the reliability index derived for the different types of loading, but with the same magnitude, is close to one another. This has also been found in Meinen and Steenbergen (2018) and (Caspeele & Van Den Hende, 2023).

Based on the derived figures, the critical corrosion degree for a singly reinforced concrete beam subjected to bending can be determined based on the loading situation. In order to do so, one needs to determine the main type of permanent G (self-weight or imposed) and variable Q (imposed, wind, traffic or snow) loading, and the load ratio $\chi = \frac{Q}{G+Q}$ between them. Note that it is assumed in this work that only one type of variable loading is dominant. As these two parameters can be easily quantified for a structure, the derived graphs enable an easy determination of the critical corrosion threshold. In general, one can conclude that for an ordinary structure corresponding to CC2 where the remaining reinforcement area A_s is considered deterministic, the critical corrosion degree varies between 10% in case of dominating permanent loads, and 30% in case of dominating variable loads. With the exception of traffic loads, where the critical corrosion degree remains constant around 10%, regardless of the ratio between the variable and permanent load.

2.2. Quantification of allowable corrosion degree as uncertain property

Commonly, the remaining reinforcement area of a corroded structure is highly uncertain as the onset of corrosion and the corrosion rate depend on a large number of physical variables which are not well known (Vořechovská et al., 2010). It is therefore crucial to take this uncertainty into account in the safety assessment of a concrete structure. In this work, the corrosion degree α is used as probabilistic quantity, which expresses the ratio between the corroded reinforcement $A_{s,corr}$ and the initial cross-sectional area $A_{s,0}$. The value of α is considered to follow a Beta distribution with boundaries at 0 and 100%, ensuring the reinforcement

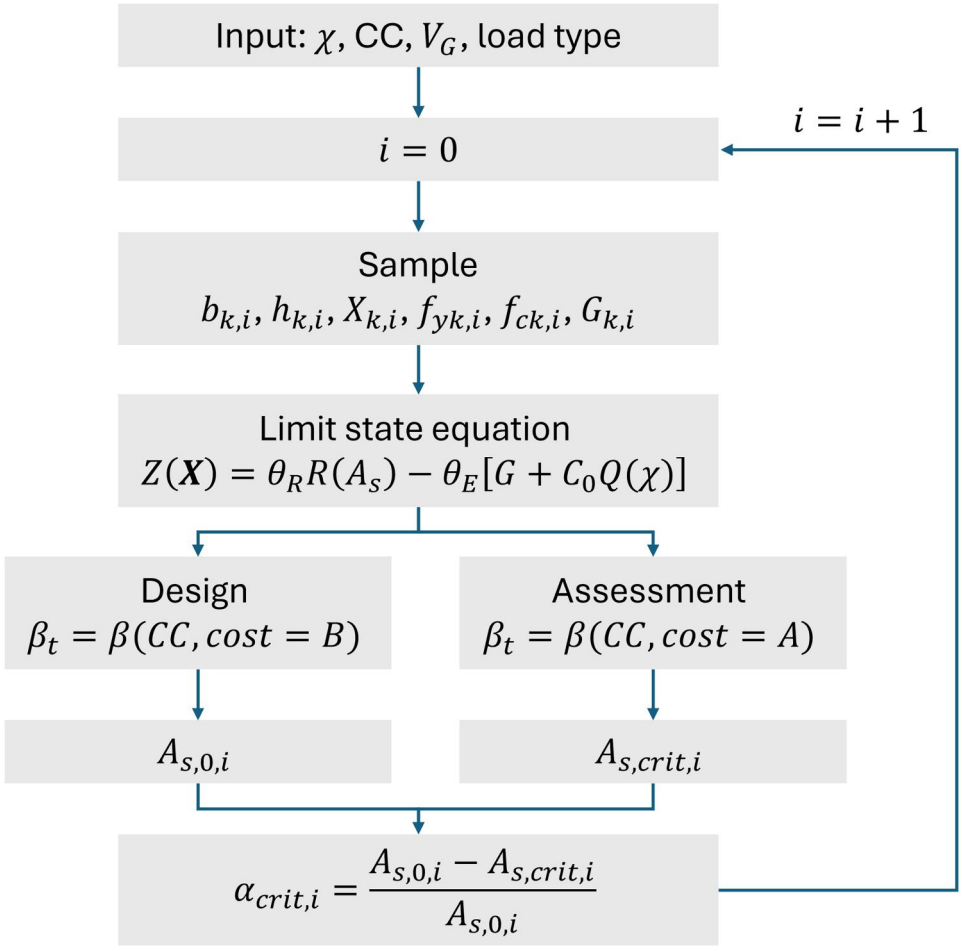

Figure 3. Flowchart for derivation of the critical corrosion degree.

area cannot drop below zero or become larger than the initial area in the uncorroded situation.

For a set of design parameters, the initial area $A_{s,0}$ that corresponds to the $\beta_{t,1y}$-value for the design of structures (cost type B) is determined as in the previous section. Afterwards, the limit state equation from Equation (1) is evaluated considering the critical corrosion degree α_{crit} that determined the area of reinforcement as well as the ultimate strain following Equation (2). Similarly as in Section 2.1, for a fixed value of the load types and load ratio χ in a situation corresponding to CC2, the characteristic values of the design parameters are varied randomly over their range defined in Table 2 by taking 100 samples (LHS). For each sample, the combinations of the mean (μ_α) and coefficient of variation (V_α) of the critical corrosion degree α_{crit}, which correspond to the $\beta_{t,1y}$-value for the assessment of existing structures (cost type A), are determined. The result is an interaction diagram for each sample, and the interaction diagrams for each of the 100 samples are given in Figure 7, where the darker colors represent a higher density in interaction diagrams.

The interaction diagram can be interpreted as follows. An existing structure is assessed and the corrosion degree is quantified, taking into account the uncertainty of the estimation. This uncertainty is translated into values for the mean μ_α and coefficient of variation V_α, which leads to a point that can be drawn on the interaction diagram. Choosing the correct diagram (considering load types and ratio of the structure), the point can for example be located at the top right of the diagram, which indicates an unsafe situation, or at the bottom left, which indicates a safe situation. The results show that a higher mean value μ_α and larger coefficient of variation V_α lead to a less safe situation. This leads to the logical conclusion that a considerable uncertainty on the remaining reinforcement area needs to be covered by a lower value of the allowable corrosion degree. Moreover, there exists a limit for the values of V_α, because values that are too large will lead to an unrealistic Beta-distribution. This will not cause an issue for the practical application, as all realistic distributions for the corrosion degree, i.e. combinations of μ_α and V_α, are included in the analysis.

Instead of using an interaction diagram for the critical corrosion degree, one could also combine the values for μ_α and V_α in a single characteristic value $\alpha_{k,crit}$, corresponding to the 95% fractile of the $Beta(\mu_\alpha, V_\alpha, 0, 100)$-distribution. Using the same sampling method described previously, the value of $\alpha_{k,crit}$ is determined, while also sampling for V_α in a range indicated by Figure 7 (e.g. between 0 and 0.11 for $\chi = 0.6$). The ranges of results corresponding to CC1, CC2 and CC3 are given in

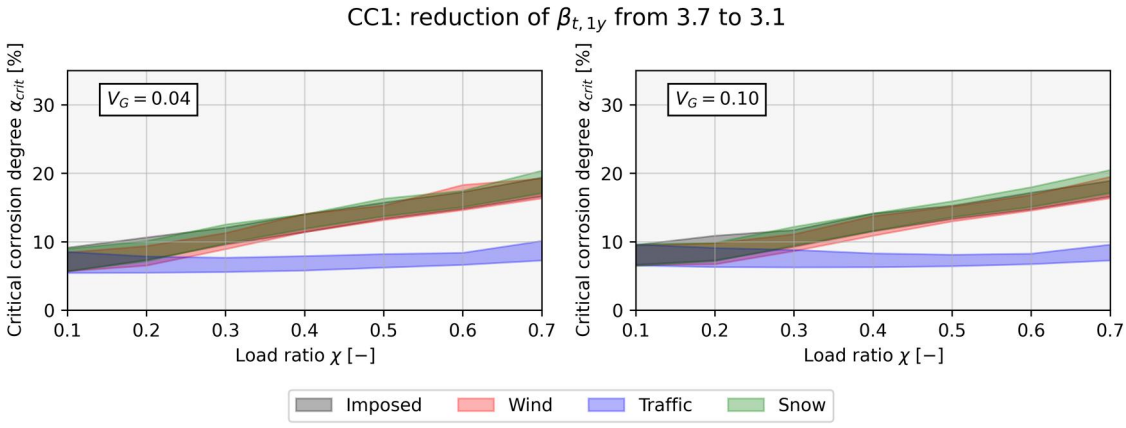

Figure 4. Critical corrosion degree as deterministic property for a range of different design situations according to CC1.

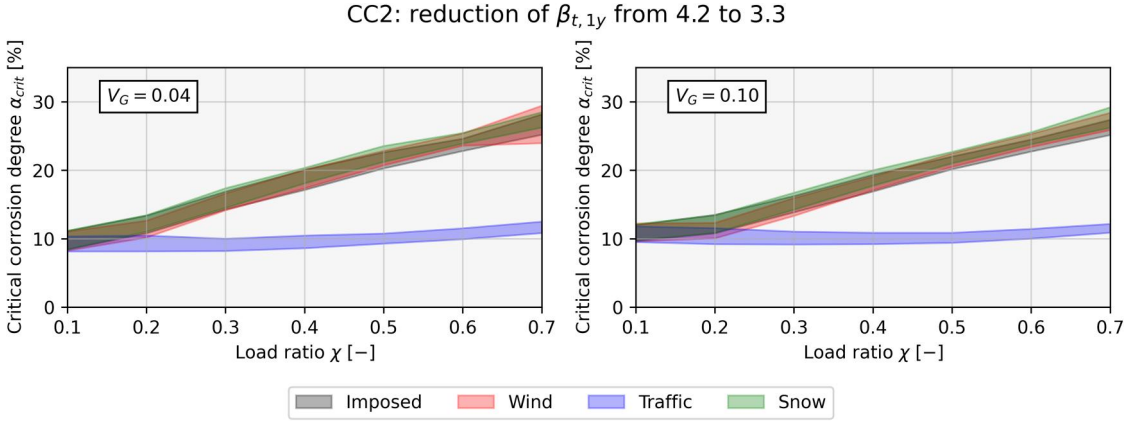

Figure 5. Critical corrosion degree as deterministic property for a range of different design situations according to CC2.

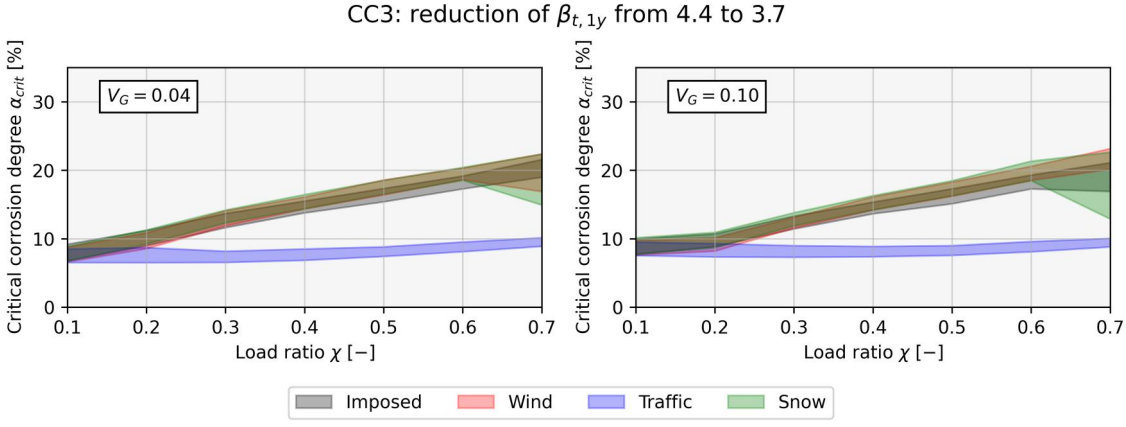

Figure 6. Critical corrosion degree as deterministic property for a range of different design situations according to CC3.

Figures 8–10, respectively. These figures are similar to the ones derived in Section 2.1, but additionally take into account the uncertainty on the corrosion level.

The graphs of the characteristic value of the critical corrosion degree $\alpha_{k,crit}$ in a probabilistic framework (Figures 8–10) lead to a wider range of results compared to the deterministic value of α_{crit} (Figures 4–6), which makes it less straightforward to choose the value for $\alpha_{k,crit}$. It is proposed to use the mean value of the results, indicated by the dotted line in the figures, which will introduce an error as the target β_t-values are not achieved exactly. To verify this approach, the variability of the reliability index β is determined when using the mean value of the critical characteristic corrosion degree $\alpha_{k,crit}$, which would ideally lead to the target reliability index β_t for existing structures. A design is considered according to the mean of the ranges given in Table 2, for a beam subjected to a wind load, a permanent load with $V_G = 0.04$ and consequence class CC2.

For this design situation and a fixed value of χ, 1000 samples of V_λ are generated which range between zero and

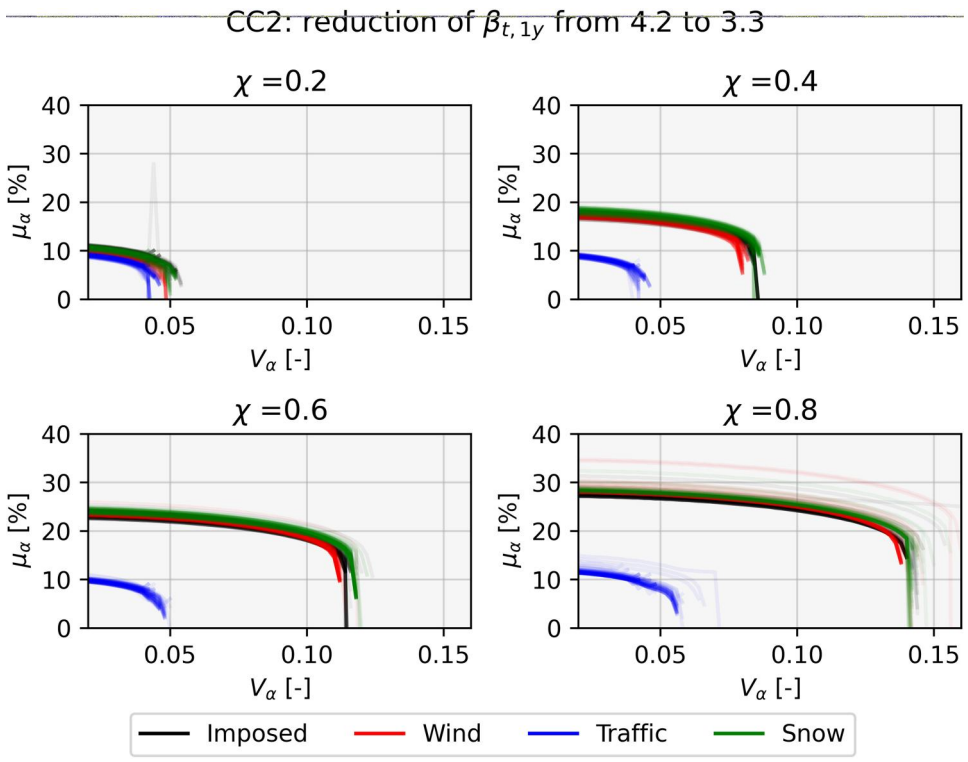

Figure 7. Interaction diagram for stochastic corrosion degree α for range of different design situations in CC2.

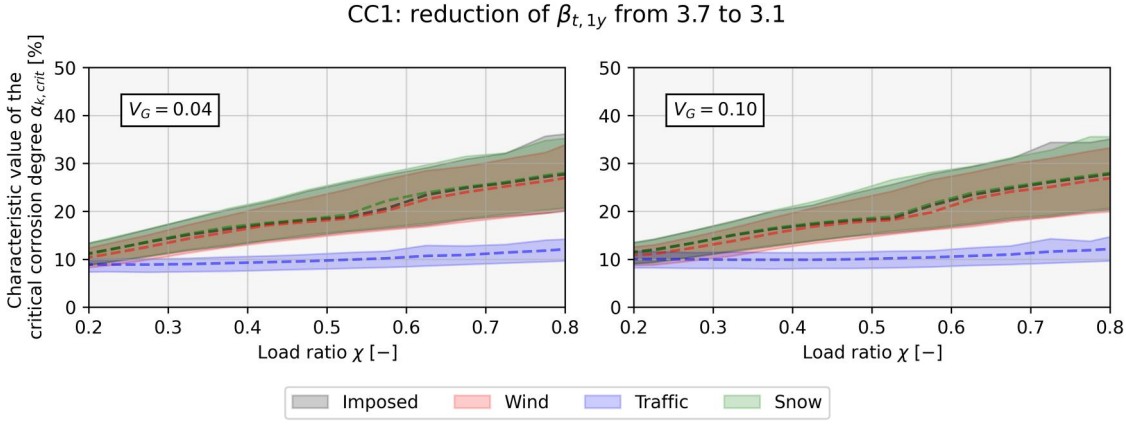

Figure 8. Characteristic value for the critical corrosion degree $\alpha_{k,crit}$ in case of CC1.

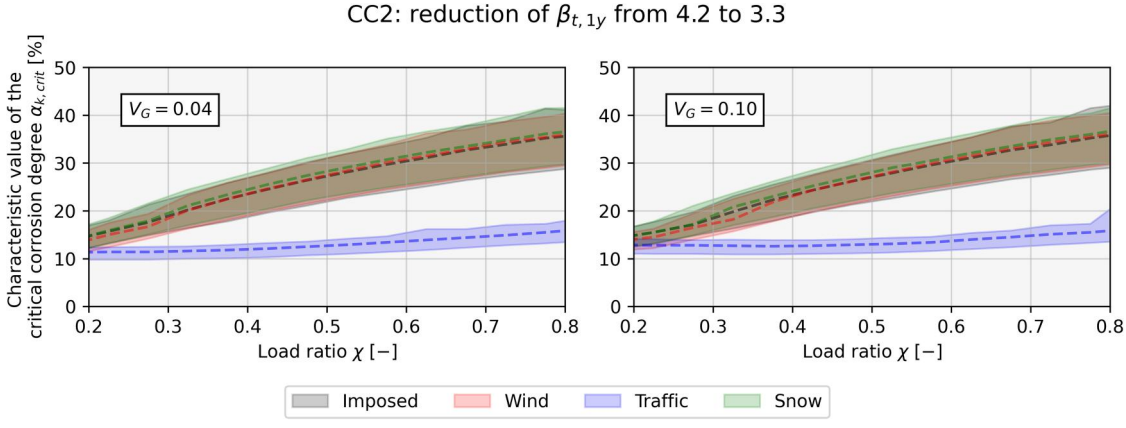

Figure 9. Characteristic value for the critical corrosion degree $\alpha_{k,crit}$ in case of CC2.

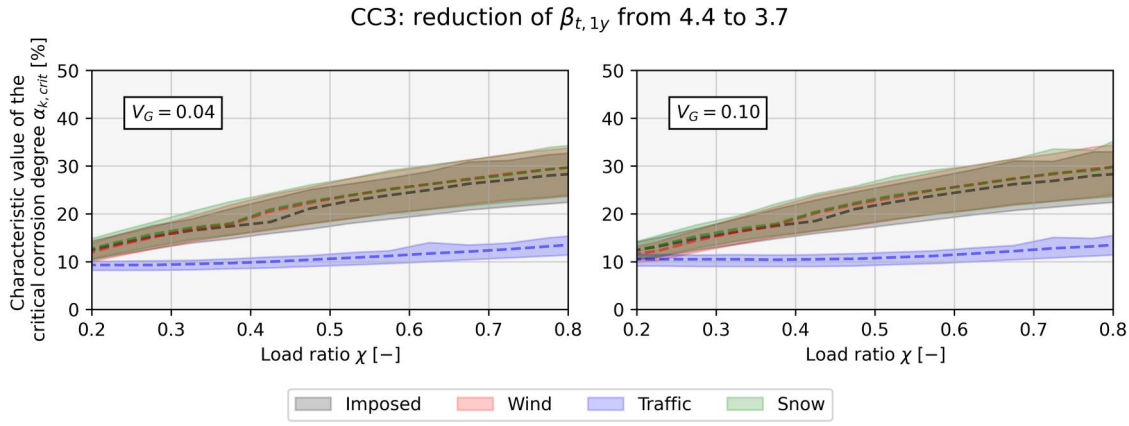

Figure 10. Characteristic value for the critical corrosion degree $\alpha_{k,crit}$ in case of CC3.

the vertical asymptote shown in Figure 7 (as function of χ). For each sample, the actual β_{1y}-value value is determined which corresponds to the characteristic critical value $\alpha_{k,crit}$ that is chosen from the dotted line in Figure 9. The results are shown in Figure 11, where the distribution of the derived reliability indices β_{1y} is plotted for different values of the load ratio χ. The derived β_{1y}-values deviate about $\pm$ 0.3 from the target value β_t. Usually, adopting the value $\alpha_{k,crit}$ will lead to a slight underestimation of the actual reliability index β_{1y}, which means the reliability level is slightly lower than expected. However, the variability around the target value remains limited when using the mean values of $\alpha_{k,crit}$ in Figure 9 (dotted line), and is similar to the error of the partial factor approach (Caspeele & Van Den Hende, 2023), which implies it is acceptable.

2.3. Application

In order to use the criterium in practice, an estimation of the corrosion degree is required. Therefore, it is required to have measurements of the corrosion degree at multiple locations of the concrete structure. There will be scatter in the results and the corrosion degree will deviate from one location to the other. Therefore, the characteristic value in terms of the 95%-interval needs to be determined. This value is ultimately compared to the critical corrosion degree derived in the previous section in order to assess the structure.

2.4. Effect of partial factors, abundance of reinforcement and changing loads

The described approach determines the critical corrosion degree for structures which have been designed according to a specific target reliability index β_t that is reached using a full-probabilistic approach. This allows one to gain insight into how a change in relative cost class (and thus reduction in β_t) is reflected in terms of required reinforcement, or in this study, the allowable corrosion level. In practice, there are a number of reasons why the reliability index β related to a specific design or assessment situation deviates from its target value. In these situations, the critical corrosion degree can be higher or lower than the values described in this work. Nevertheless, this work proposed generalized results without case-specific differences and can be used as a reference for the critical corrosion degree for a wide range of structures. A number of practical situations where the critical corrosion degree might deviate from the current findings are elaborated.

In many practical situations, the reinforcement has been designed based on the partial factor method, which induces a difference between the actual reliability index β and the target value β_t. As investigated in the work of Caspeele and Van Den Hende (2023), depending on the specific load ratio χ, this means that the actual reliability index is either higher (low values of χ) or lower than the target value (high values of χ). As a result, the reinforcement area is respectively over- or underdesigned for each situation. Secondly, the placed amount of reinforcement is in reality larger than the designed amount (due to the selection of the number and diameter of the rebars), which leads to a safer structure. According to the elaborated approach, this allows for more corrosion before the situation becomes critical. Lastly, the loads applied to the structure can change over time. In case the load increases with time, the critical corrosion degree derived in this work is an overestimation and vice-versa. For structures where the loads evolve significantly over time, such as bridges, this is important to take into account.

3. Prediction of characteristic corrosion degree in time

Given the maximum corrosion degree derived in the previous part of this work, an existing structure can be assessed by predicting the evolution in time of the corrosion degree. This is done based on the onset of corrosion and corrosion rate, considering their associated uncertainties. In this section, the corrosion degree in terms of the characteristic value α_k is quantified for a range of cement types and exposure conditions, for both chloride- and carbonation-induced corrosion. Consequently, the predicted values of α_k (whereby the characteristic value of the corrosion degree equals zero during the initiation period and increases over the propagation period) are compared to the critical value $\alpha_{k,crit}$, derived in the first part of this work, and the remaining lifetime of the structure is predicted. The applied equations for the durability and structural behavior of concrete structures that are used in this

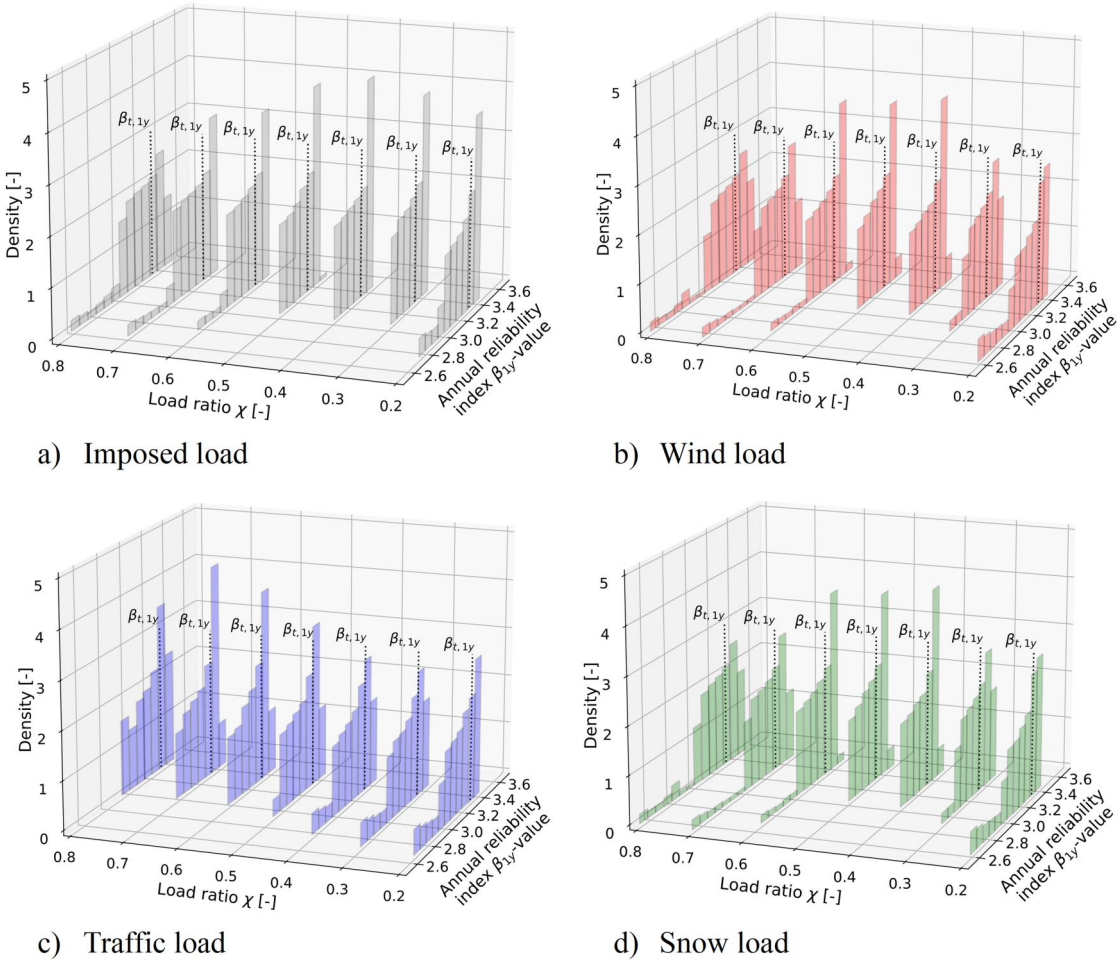

Figure 11. Distribution of annual β_{1y}-values corresponding to critical characteristic values related to CC2.

part have been studied extensively in the past and are generally agreed upon. The goal of this section is to apply the equations for a range of different cases, which enables a practical assessment of the corrosion risk for a broad range of structures in case no additional information is available.

3.1. Prediction of chloride-induced corrosion

In case of chloride-induced corrosion, the corrosion process is considered to start at the instant in time where the chloride concentration, described by the diffusion law, reaches a critical threshold C_{crit}. Based on the generally accepted approach described in Schiessl (2006), the initiation period T_{ini} (i.e. end of depassivation and start of corrosion phase if humidity and oxygen are present) is determined by:

$$T_{ini} = \left[\frac{X\text{-}\Delta x}{2\sqrt{D_0 t_0^{\alpha}}} \frac{1}{\mathrm{erf}^{-1}\left(1 - \frac{C_{crit}}{C_s}\right)} \right]^{\frac{2}{1-\alpha}} \tag{4}$$

Where D_0 is the initial diffusion coefficient at $t_0 = 28$ days, α is the aging coefficient of the diffusion coefficient, C_s the surface concentration and X the concrete cover. The parameter Δx takes into account that at the surface of the concrete substrate, the so-called convection zone, the chloride profile might differ from the solution of the diffusion law.

When the reinforcement steel becomes depassivated (i.e. at $t = T_{ini}$), the radius loss r_{corr} due to corrosion increases (on average) linearly with time:

$$r_{corr} = V_{corr} \cdot [t - T_{ini}] \tag{5}$$

Where V_{corr} is the corrosion rate. Chloride-induced corrosion typically appears in the form of local corrosion pits. Linking the radius loss with the loss of reinforcement area is an important aspect, which can be simulated based on models simulating the microstructure behavior of the pits in detail (Lim et al., 2016; Zhao et al., 2016). However, in order to be able to evaluate the pitting corrosion in an efficient and practically applicable way, analytical models have been derived in literature to relate this pit depth to the total loss of rebar area (Val & Melchers, 1997; Yuan & Ji, 2009). In this work the analytical model of Val and Melchers (1997) is used, which assumes a hemispherical pit shape:

$$\frac{A\left(\frac{r_{corr}}{D_0}\right)}{A_0} = \begin{cases} 1 - A_1 - A_2, & \frac{r_{corr}}{D_0} \le \frac{\sqrt{2}}{2} \\ A_1 - A_2, & \frac{\sqrt{2}}{2} < \frac{r_{corr}}{D_0} \le 1 \\ 0, & \frac{r_{corr}}{D_0} > 1 \end{cases} \tag{6}$$

With:

$$A_1 = \frac{1}{\pi}\left[arcsin\left(2\frac{r_{corr}}{D_0}\sqrt{1-\left(\frac{r_{corr}}{D_0}\right)^2}\right) - \frac{r_{corr}}{D_0}\sqrt{1-\left(\frac{r_{corr}}{D_0}\right)^2}\left|2-4\left(\frac{r_{corr}}{D_0}\right)^2\right|\right] \quad (7)$$

$$A_2 = \frac{4}{\pi}\left(\frac{r_{corr}}{D_0}\right)^2\left[arcsin\left(\sqrt{1-\left(\frac{r_{corr}}{D_0}\right)^2}\right) - \frac{p}{D_0}\sqrt{1-\left(\frac{r_{corr}}{D_0}\right)^2}\right] \quad (8)$$

Where A_0 is the initial reinforcement area of a bar with diameter D_0.

For all of the above-mentioned parameters, a stochastic distribution has been determined in literature, depending on the exposure type and material considered, as shown in Table 5,

Tables 6 and 7. Note that for the diffusion coefficient, the values are determined from a Rapid Chloride Migration (RCM) test, which are translated to the actual diffusion coefficient using an environmental variable, which is in this work considered to be equal to one (ambient conditions).

Table 5. Statistical characteristics chloride-induced corrosion parameters independent of material or exposure classification (fib Model Code 2020, 2024; Gehlen, 2015).

Variable	Distribution	μ	V
Concrete cover $a[mm]$*	Gamma	varying	0.17
Critical concentration $C_{crit}[m\%cement]$	Beta*	0.6	0.25

*With lower limit 0.2 and upper limit 2.0.

Table 6. Statistical characteristics chloride-induced corrosion parameters for different exposure classes (fib Model Code 2020, 2024; Gehlen, 2015).

Variable	Exposure class	Distribution	μ	V
Surface concentration $C_s[m\%cement]$	XD1	Lognormal	1.0	0.75
	XD2, XD3	Lognormal	3.0	0.75
	XS1	Lognormal	1.5	0.45
	XS2	Lognormal	3.0	0.25
	XS3	Lognormal	3.0	0.45
Depth convection zone $\Delta x[mm]$	XD1, XD2, XS1, XS2	Deterministic	0.0	/
	XD3, XS3	Beta*	10.0	0.50
Corrosion rate $V_{corr}[\mu m/y]$	XD1	Weibull	4	1.50
	XD2	Weibull	30	1.50
	XD3, XS1	Weibull	30	1.35
	XS2	Weibull	10	1.35
	XS3	Weibull	70	1.40

*With lower limit 0 and upper limit 50 mm.

Table 7. Statistical characteristics chloride-induced corrosion parameters for different material types (Gehlen, 2015).

Variable	Material	Distribution	μ	V
Initial diffusion coefficient concrete $D_0[10^{-12}m^2/s]$	CEM I	Lognormal	10.0	0.20
	CEM II/A-D	Lognormal	4.5	0.20
	CEM III/A	Lognormal	3.9	0.20
	CEM III/B	Lognormal	1.9	0.20
Aging exponent $\alpha[-]$	CEM I	Beta*	0.3	0.40
	CEM II/A-D	Beta*	0.4	0.40
	CEM III/A	Beta*	0.4	0.45
	CEM III/B	Beta*	0.45	0.44

*With lower limit 0 and upper limit 1.

Using the previously mentioned equations, the corrosion degree, i.e. fraction of the corroded reinforcement area, can be quantified over time.

The results are given in Figure 12, where the influence of the different exposure classes and cement types is investigated for a concrete structure with reinforcement diameter of 12 mm. The dominating factor is the exposure class, which may give rise to a very slow decrease in reinforcement area for exposure class XD1 and XS2, or a very rapid decrease for XS3. The parameter with the most influence is the corrosion rate V_{corr}, which is for XS3 considerably higher than for the other exposure classes. The type of cement used does not have a significant influence for XD1, XS2 or XS3, as these exposure classes represent extreme cases where the corrosion process goes either very fast or very slow. However, for the other exposure classes, the type of cement has a more significant influence on the increase of α_k over time.

3.2. Prediction of carbonation-induced corrosion

In a similar way, the corrosion degree of the reinforcement can be quantified for carbonation-induced corrosion. In this case, the corrosion process starts in case the carbonation front reaches the reinforcement, and thus the initiation period T_{ini} can be described as (ISO 16204, 2012):

$$T_{ini} = \left[\frac{X}{k_{NAC}t_0^w\sqrt{k_e k_c k_a}}\right]^{\frac{2}{1-2w}} \quad (9)$$

With:

$$w = \frac{(p_{sr}ToW)^{b_w}}{2} \quad (10)$$

$$k_e = \left(\frac{1-\left(\frac{RH_{real}}{100}\right)^{f_e}}{1-\left(\frac{RH_{ref}}{100}\right)^{f_e}}\right)^{g_e} \quad (11)$$

$$k_a = \frac{C_a}{C_l} \quad (12)$$

Where $k_{NAC}[mm/y^{0.5}]$ is the carbonation rate in standard test conditions, which is transferred to the actual carbonation rate by additional constants. k_e is the constant taking into account the environmental condition in terms of relative humidity, while k_a takes into account the actual CO_2-concentration of the concrete structure, compared to the laboratory tests. k_c is the constant taking into account the curing behavior of the concrete, which is equal to 1 as the curing time is considered to be 7 days. The value of w takes into account the effect of wetting events that might occur and inhibit further ingress of CO2. It is determined by the time of wetness $ToW[-]$, probability of driving rain p_{sr} $[-]$ and regression exponent $b_w[-]$. The value of t_0 is equal to $0.0767y$.

The distributions of all parameters are given in Tables 8–10 depending on the environmental class and cement type that is used. Note that the values for environmental class XC1 are not included, as the corrosion rate is typically

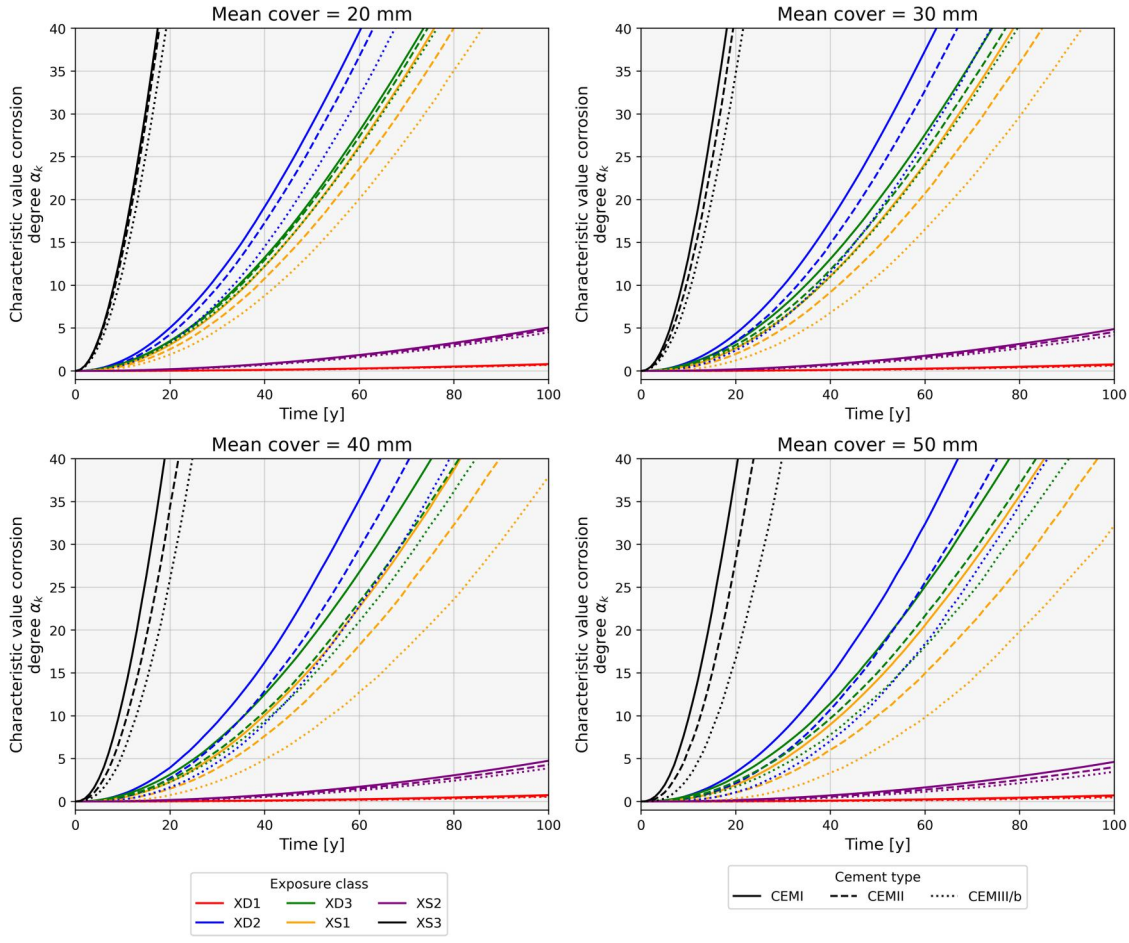

Figure 12. Prediction of the characteristic value of the corrosion degree α_k due to chloride-induced corrosion for different exposure classes and cement types; considering a rebar diameter of 12 mm.

Table 8. *Statistical characteristics carbonation-induced corrosion parameters independent of material or exposure classification (*Schiessl, 2006*;* von Greve-Dierfeld & Gehlen, 2016*).*

Variable	Distribution	μ	*V*
Concrete cover $a[mm]$	Gamma	varying	0.17
Reference relative humidity $RH_{ref}[\%]$	Deterministic	65	/
Exponent $f_e[-]$	Deterministic	5.0	/
Exponent $g_e[-]$	Deterministic	2.5	/
CO2 concentration laboratory C_l $[vol\ \%]$	Deterministic	0.04	/
CO2 concentration atmosphere C_a $[vol\ \%]$	Lognormal	0.0465	0.11
Regression exponent $b_w[-]$	Lognormal	0.446	0.37

Table 9. *Statistical characteristics carbonation-induced corrosion parameters for different exposure classes* (fib Model Code 2020, 2024*;* von Greve-Dierfeld & Gehlen, 2016).

Variable	Exposure class	Distribution	μ	*V*
Ambient relative humidity $RH_{real}[\%]$	XC2	Deterministic	95	/
	XC3, XC4	Weibull*	80**	0.13
Time of wetness $ToW[-]$	XC2	Deterministic	0.4	/
	XC3	Deterministic	0.0	/
	XC4	Deterministic	0.25b	/
Probability of driving rain p_{sr}	XC2, XC3	Deterministic	0.0	/
	XC4	Deterministic	0.35	/
Corrosion rate $V_{corr}[\mu m/y]$	XC2	Weibull	4	1.5
	XC3	Weibull	2	1.5
	XC4	Weibull	5	1.75

*min = 0; max = 100.
**Environmental conditions expected in Great Britain, The Netherlands, Germany, Denmark and Norway.

considered negligible and thus no corrosion will occur. The parameters which are prescribed in literature (fib Model Code 2020, 2024, 2006; von Greve-Dierfeld & Gehlen, 2016) to follow a normal distribution are transferred to a lognormal distribution with the same mean μ and standard deviation σ to ensure non-zero values.

After the initiation phase, the propagation phase starts and the corrosion penetration depth r_{corr} evolves linearly with time, similar to the case of chloride-induced corrosion, as described by Equation (5). However, for carbonation-induced corrosion, typically no pits are formed but the radius of the reinforcement bar is reduced by r_{corr}. Thus, the relation between the remaining reinforcement area and the penetration depth is described as:

$$A(r_{corr}) = \pi\left(\frac{D_0}{2} - r_{corr}\right)^2 \tag{13}$$

The resulting predictions of the characteristic value of the corrosion degree α_k for the different exposure classes and cement types are given in Figure 13. Compared to the results from the chloride-induced corrosion, the corrosion degree increases significantly slower for carbonation-induced corrosion, which is expected as carbonation-induced corrosion is typically a slower (more widespread) process. It is shown that the behavior of the carbonation induced corro-

sion degree typically follows a linear behavior, whereas the chloride induced corrosion is nonlinear. This is caused by their different relationship between the (linearly increasing) pit depth and the loss of area, described by either Equations (6) or (13).

The different cement types considered do not significantly influence the predicted α_k, except for very large initiation periods. Similar to the case of chloride-induced corrosion, the main influence is the exposure class. The most severe exposure class is XC4, which also has the largest corrosion rate V_{corr}. Whether XC2 or XC3 is more critical depends on the specific situation, as XC2 has a larger corrosion rate V_{corr}, but also a longer initiation period T_{ini}.

3.3. Influence of reinforcement diameter

A final important parameter that needs to be considered is the influence of the rebar diameter, which is investigated in Figures 14 and 15 for chloride- and carbonation induced corrosion, respectively. It is shown that a smaller rebar diameter gives rise to a more pronounced decrease in cross-sectional area, and hence a somewhat increased sensitivity to corrosion. A larger rebar diameter can significantly slow down the increase of α_k, which is an aspect that could be taken into account in the design of the concrete element. Moreover, this shows that the rebar diameter also needs to be considered explicitly when assessing the time-dependent reliability of a degrading concrete structure. Further, the effect that the rebar diameter might have on the development of cracks in the concrete needs to be emphasized. It was found that a larger diameter might slow down the increase in corrosion in uncracked state, however it typically increases the formed crack width in case the concrete cracks (Martens et al., 2022). This shows that a larger rebar does not necessarily lead to a safer situation.

Table 10. *Statistical characteristics carbonation-induced corrosion parameters for different material types (*von Greve-Dierfeld & Gehlen, 2016*).*

Variable	Material	Distribution	μ	*V*
Carbonation rate $k_{NAC}[mm/y^{0.5}]$	CEM I	Lognormal	3.3	0.33
	CEM II/A	Lognormal	3.7	0.27
	CEM II/B	Lognormal	4.7	0.23

3.4. Defining the end of lifetime of a structure

The structural capacity-related end of lifetime of a structure is defined as the point in time where the characteristic value of the corrosion degree α_k becomes higher than the critical value $\alpha_{k,crit}$. Based on this principle, the remaining lifetime of a structure can be predicted in a quantitative way. The

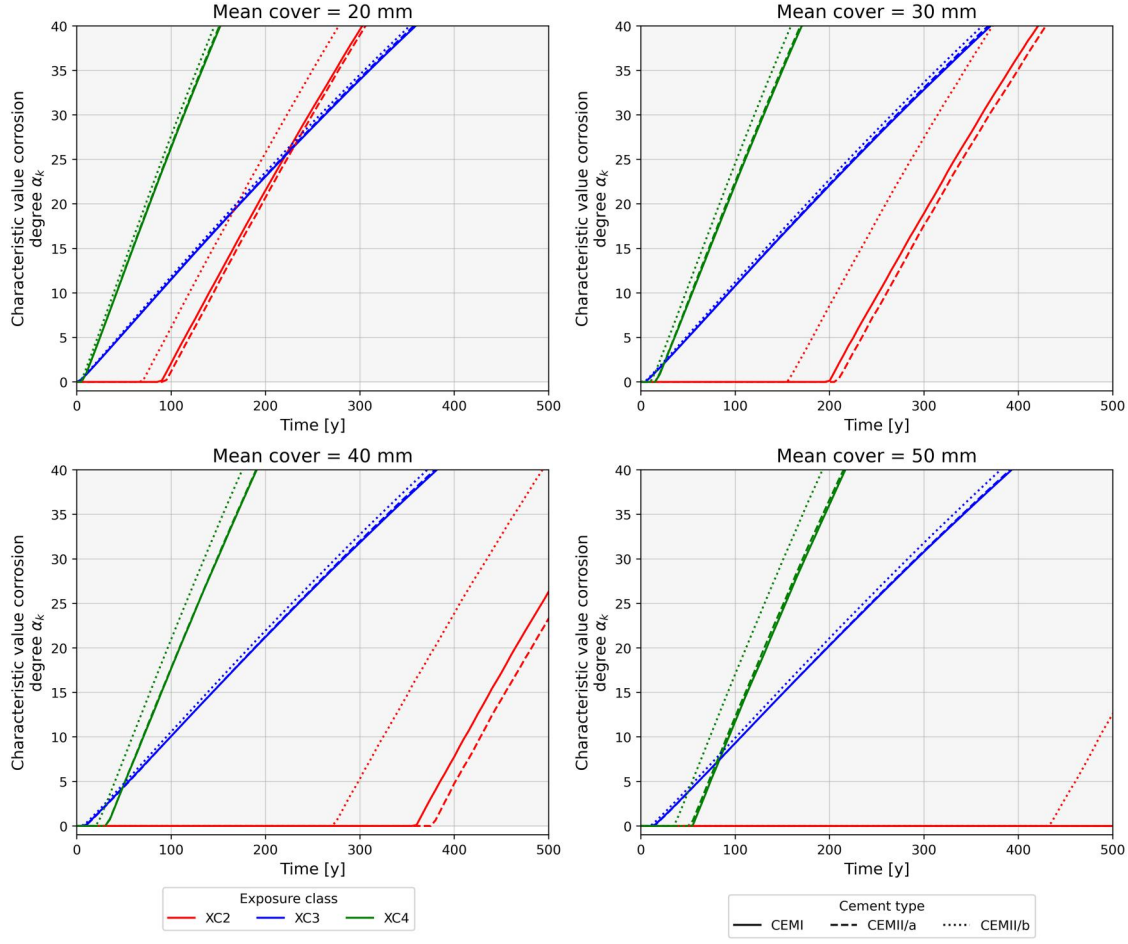

Figure 13. Prediction of the characteristic value of the corrosion degree α_k due to carbonation-induced corrosion for different exposure classes and cement types; considering a rebar diameter of 12 mm.

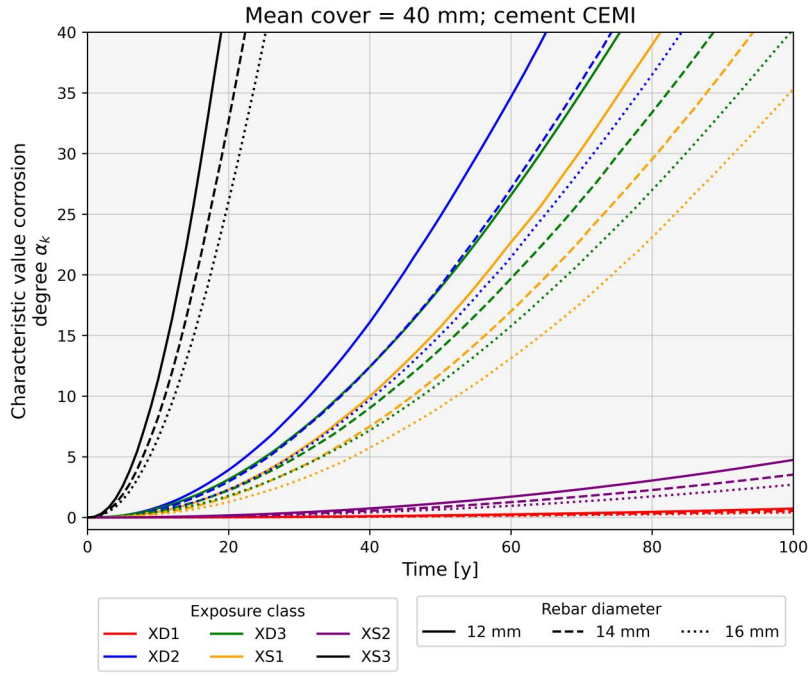

Figure 14. Prediction of the characteristic value of the corrosion degree α_k due to chloride-induced corrosion for different exposure classes and rebar diameters; considering CEMI and a mean cover of 40 mm.

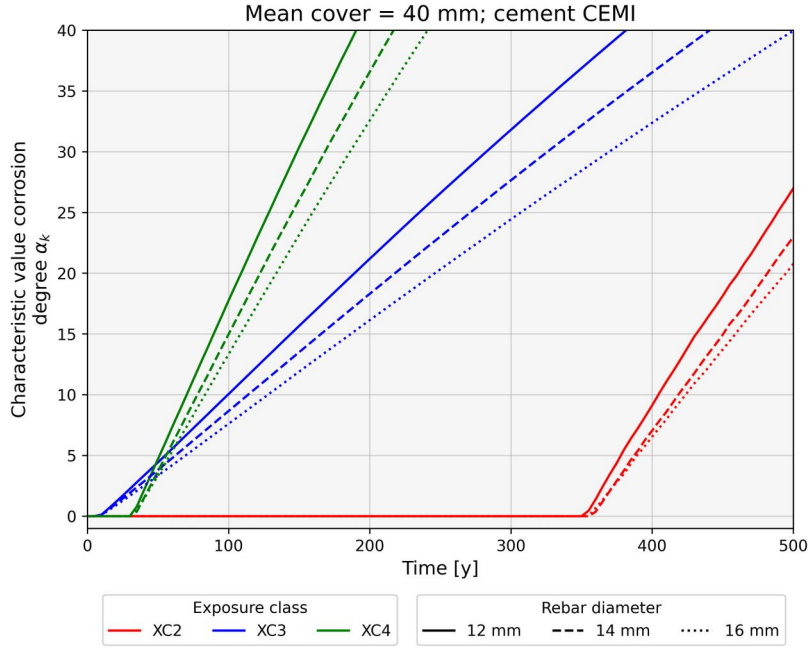

Figure 15. Prediction of the characteristic value of the corrosion degree α_k due to carbonation-induced corrosion for different exposure classes and rebar diameters; considering CEMI and a mean cover of 40 mm.

lifetime of the structure can be determined based on 7 parameters. In the first part, it was shown that the value for $\alpha_{k,crit}$ mainly depends on the load ratio χ, the type of variable loading and the consequence class. For the prediction of α_k over time, the main influencing parameters are the exposure class, concrete cover, reinforcement diameter and cement type (the latter not being very important for carbonation-induced corrosion).

As an illustration, the methodology is shown in Figure 16 for a reinforced concrete beam of CC2 subjected to imposed load with a load ratio χ of 0.6, corresponding for example to an element in an industrial storage building (Sykora, 2015). Using Figure 9, this leads to a value for $\alpha_{k,crit}$ of 30%. Consider that the concrete beam is permanently in contact with industrial water and is exposed to chlorides classified in exposure class XD2, a CEMI based concrete, a mean concrete cover of 40 mm and reinforcement diameter of 16 mm. At an age of 55 years, the value of α_k becomes higher than $\alpha_{k,crit}$. At this point (indicated as end of lifetime in Figure 16), the safety level of the element can be considered to become critical and an intervention is required.

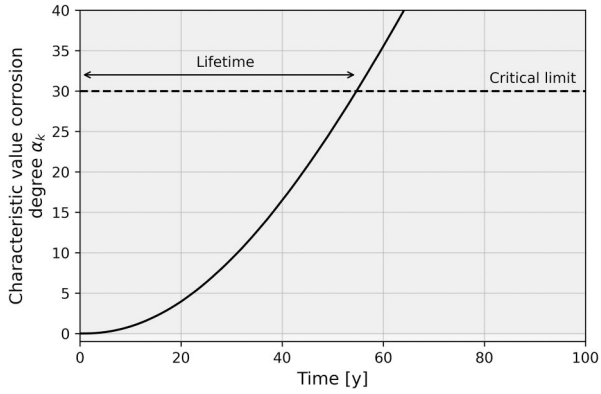

Figure 16. Determination of structural end of lifetime using proposed framework.

This example shows how the results presented in Sections 2, 3.1 and 3.2 are coupled to determine a structural safety-related lifetime of a structure. When no additional information from measurements or the design phase is available (e.g. chloride measurement, cover measurements, …), the derived graphs from Sections 2 and 3 can be used to estimate the reliability-based structural end of lifetime.

4. Discussion

To assess the structural reliability of a corroding structure over its intended lifetime, a criterium based on a characteristic value of the critical corrosion degree $\alpha_{k,crit}$ is proposed. The criterium is defined for a wide range of practical cases and $\alpha_{k,crit}$ can be easily obtained from the results in the previously presented figures. However, the value of $\alpha_{k,crit}$ is currently only quantified for a simply supported singly reinforced beam with rectangular cross section that is subjected to bending and the approach also needs to be further extended to different type of structural elements (slabs and columns) and different types of internal forces (shear and compression).

Based on information from literature, a prediction over time of the characteristic corrosion degree can be obtained considering the type of cement, average concrete cover, exposure class and rebar diameter. The resulting predicted values of α_k can be compared with the critical values $\alpha_{k,crit}$ which, on their turn, mainly depend on the load ratio, type of variable loading and consequence class. Combining these two aspects, a prediction of the structural lifetime can be done based on the instant where $\alpha_{k,crit}$ is reached. This opens the possibility to design e.g. the necessary concrete cover, based on the fact that $\alpha_{k,crit}$ may not be exceeded within the intended lifetime. This results in a well-defined criterium for the durability design of a concrete element based on safety aspects, without the need to work out a proxy criterion for corrosion initiation only. Such a proxy criterion for corrosion initiation is currently common practice and uses target reliability indices given by (CROW, 2018; EN1990 Eurocode, 2002; ISO, 2015; LNEC E 465, 2007; NEN 6700 TGB 1990, 2005; Schiessl, 2006) and summarized in Gehlen (2015), which propose a limit to the probability of depassivation and thus only focusses on the initiation period. The target reliabilities for depassivation have a large variation depending on which source is considered and generally lack a fundamental link with the safety of the structure, which is solved with the approach proposed in this work.

In the new fib Model Code 2020, 2024, a different approach is proposed where no longer the probability of depassivation is used, but a maximum penetration depth of the corrosion products. Based on results from literature (Alonso et al., 1998; Hunkeler, 2006; Parrott, 1990; Tuutti, 1982), this maximum penetration depth is fixed at the instant in time where corrosion-induced cracks are formed, but does not consider the ultimate limit state. The research proposed in this work supplements the approach from fib Model Code 2020, 2024 by proposing a criterium based on the limit for the structural reliability, instead of corrosion-induced damage. Both criteria can be used to assess an existing structure, predicting both the expected damage and structural reliability. The approach considered in this work can be used for a preliminary assessment of a corroding structure, where the derived criterium gives an indication of how critical a corrosion state can be. This information is useful to decide on the need for a more in-depth assessment of the structure, especially in cases when a large number of structures have to be assessed and one has to make a decision about the prioritization of such in-depth assessments and interventions.

The critical corrosion degree can also be determined with the semi-probabilistic partial factor method instead of a full probabilistic analysis. Although a partial-factor based approach will make the calculation procedure more straightforward, it will lead to an erroneous result as the design (or assessment) with the partial factor approach inherently induces an additional deviation to the target reliability level. By using a full-probabilistic approach, it is possible to match the change in target reliability with a specific case-specific allowable corrosion degree.

The allowable critical corrosion degree is based on the principle of a reduced target reliability index for existing structures, based on economic optimization. Generally, the target reliability for economic optimization is more stringent than the reliability level required for human safety. However, for some cases (especially in CC3), it is possible that the human safety criterium is governing compared to the economical aspect. In that case, the corrosion limit derived in this work cannot be applied and should be adjusted. For more information regarding the derivation of a target reliability index for human safety is referred to (Caspeele et al., 2016; fib Model Code 2020, 2024; Fischer et al., 2019; Pandey et al., 2024; Tanner & Hingorani, 2015; Trbojevic, 2009; Vrijling et al., 2013).

This work focusses on the time until an intervention (e.g. maintenance) is required by deriving the instant in time when a lower value of the target reliability is reached, but does not focus on the maintenance action itself. When the reliability limit, or critical corrosion level, is reached an essential maintenance intervention is required. One proposal is to stop the corrosion process by applying cathodic

protection and thus maintaining the same reliability level over time (Julio, 2022A). Another option would be to apply structural strengthening such as FRP or external reinforcement (Julio, 2022b).

5. Conclusions

This study presents a comprehensive approach for assessing the maximum corrosion degree, taking into consideration the specific consequence class. A novel criterion is introduced, based on the allowable loss of reinforcement area when comparing the target reliability indices for new and existing structures. The results are presented in figures which enable to determine the critical corrosion degreeof a structure in a straightforward way, considering its load ratio, type of variable loading and consequence class. Values for the critical corrosion degree are proposed for a range of different structures that can be used to assess an existing structure in case information regarding the corrosion degree is collected (with or without uncertainty). In addition, the corrosion degree can be predicted over time which allows to define the end of lifetime, corresponding to the point in time when the critical corrosion degree is reached.

This easy-to-use criterium allows to integrate principles of structural reliability into the corrosion prediction of the structure. This is in contrast with current practice which is commonly based on durability calculations alone that propose a limit for the probability of depassivation, which is serving as a proxy but does not allow to assess the ultimate limit state in due consideration of active corrosion. Based on probabilistic models proposed in the literature, the prediction of the corrosion degree for a range of different exposure classes, cement types, concrete covers and rebar diameters is performed for structures subjected to either chloride- or carbonation-induced corrosion.

For typical reinforced concrete beams the load ratio χ of variable to total loading is in the range of 0.4–0.6 (Sykora, 2015). For these structures, the critical characteristic corrosion degree is around 10–12% for structures subjected to traffic load, and does not change with the consequence class. For other types of loading such as wind, snow or imposed loads, the critical characteristic corrosion degree is around 17–26%. For the latter types of loading, the critical corrosion degree is more dependent on the load ratio and consequence class.

In general, the larger the load ratio, the larger the critical corrosion degree. However, in terms of consequence class, there is no clear trend. It is shown that structures subjected to traffic loads have a significantly lower critical corrosion degree, compared to structures subjected to other types of variable loading. This is due to the fact that the uncertainty regarding the load induced by traffic is generally much lower than for other load cases, causing the uncertainty on the resistance, which is altered by corrosion, to have a relatively higher impact to the structural reliability compared to other load cases. Further work includes the extension of the corrosion limits for other types of structures such as columns and plates.

Disclosure statement

No potential conflict of interest was reported by the author(s).

Funding

This research was performed within the framework of FWO SBO project lifeMACS "Multi-layer Bayesian life-cycle Methodology for the Assessment of Existing Concrete Structures," supported by FWO-Flanders [FWO-SBO project S001021N].

ORCID

Karel Van Den Hende http://orcid.org/0000-0002-3265-9868
Wouter Botte http://orcid.org/0000-0003-1355-1517
Stijn Matthys http://orcid.org/0000-0002-9588-8561
Geert Lombaert http://orcid.org/0000-0002-9273-3038
Robby Caspeele http://orcid.org/0000-0003-4074-7478

Data availability statement

Data sharing is not applicable to this article as no new data were created or analyzed in this study.

References

Alexander, M., & Beushausen, H. (2019). Durability, service life prediction, and modelling for reinforced concrete structures – review and critique. *Cement and Concrete Research*, *122*, 17–29. https://doi.org/10.1016/j.cemconres.2019.04.018

Allen, D. E. (1991). Limit states criteria for structural evaluation of existing-buildings. *Canadian Journal of Civil Engineering*, *18*(6), 995–1004. https://doi.org/10.1139/l91-122

Alonso, C., Andrade, C., Rodriguez, J., & Diez, J. M. (1998). Factors controlling cracking of concrete affected by reinforcement corrosion. *Materials and Structures*, *31*(7), 435–441. https://doi.org/10.1007/BF02480466

Aslani, F., & Dehestani, M. (2020). Probabilistic impacts of corrosion on structural failure and performance limits of reinforced concrete beams. *Construction and Building Materials*, *265*, 120316. https://doi.org/10.1016/j.conbuildmat.2020.120316

Azad, A. K., Ahmad, S., & Al-Gohi, B. H. A. (2010). Flexural strength of corroded reinforced concrete beams. *Magazine of Concrete Research*, *62*(6), 405–414. https://doi.org/10.1680/macr.2010.62.6.405

Azher, S. A. (2005). *A prediction model for the residual flexural strength of corroded reinforced concrete beams* [Thesis]. King Fahd University of Petroleum & Minerals.

Bagheri, M., Hosseini, S. A., Keshtegar, B., Correia, J. A. F. O., & Trung, N.-T. (2020). Uncertain time-dependent reliability analysis of corroded RC structures applying three-term conjugate method. *Engineering Failure Analysis*, *115*, 104599. https://doi.org/10.1016/j.engfailanal.2020.104599

Caspeele, R., Steenbergen, R., & Sykora, M. (2016). *fib Bulletin 80 Partial factor methods for existing concrete structures*. FIB.

Caspeele, R., & Van Den Hende, K. (2023). Validation of the harmonized partial factor method for design and assessment of concrete structures as proposed for fib model code 2020. *Structural Concrete*, *24*(4), 4368–4376. https://doi.org/10.1002/suco.202201109

CROW. (2018). *CUR-Aanbeveling 121:2018 Bepaling ondergrens verwachte levensduur van bestaande gewapende betonconstructies*. CUR.

Diamantidis, D., & Bazzurro, P. (2014). *Safety acceptance criteria for existing structures* [Paper presentation]. Workshop on Risk Acceptance and Risk Communication, Stanford, CA.

EN1990 Eurocode. (2002). *Basis of structural design*. EN.

EN1992 Eurocode. (2004). *Design of concrete structures - Part 1-1: General rules and rules for buildings*. EN.

fib Model Code 2020. (2024). *Lausanne: International Federation for Structural Concrete*. FIB.

Fischer, K., Viljoen, C., Köhler, J., & Faber, M. H. (2019). Optimal and acceptable reliabilities for structural design. *Structural Safety*, *76*, 149–161. https://doi.org/10.1016/j.strusafe.2018.09.002

Gehlen, C. (2015). *fib Bulletin 76 Benchmarking of deemed-to-satisfy provisions in standards: Durability of reinforced concrete structures exposed to chlorides*. FIB.

Hunkeler, F. (2006). *Risk of spalling of concrete due to rebar corrosion (in German)*.

ISO 16204 (2012). *ISO16204: Durability - Service life design of concrete structures*. ISO.

ISO 2394 (2015). *ISO2394: General principles on reliability for structures*. ISO.

JCSS. (2000). *Probabilistic model code part 1 - basis of design*. JCSS.

Julio, E. (2022a). *fib Bulletin 102 Guide for protection and repair of concrete structures*. FIB.

Julio, E. (2022b). *fib Bulletin 103 Guide for strengthening of concrete structures*. FIB.

Lim, S., Akiyama, M., & Frangopol, D. M. (2016). Assessment of the structural performance of corrosion-affected RC members based on experimental study and probabilistic modeling. *Engineering Structures*, *127*, 189–205. https://doi.org/10.1016/j.engstruct.2016.08.040

LNEC E 465 (2007). *LNEC E 465 Concrete – methodology for estimating the concrete performance properties allowing to comply with the design working life of reinforced or prestressed concrete structures under environmental exposures XC and XS*.

Markova, J., Holicky, M., Jung, K., & Sykora, M. (2017). Basis for reliability assessment of industrial heritage buildings and a case study of a 19th century factory. *International Journal of Heritage Architecture: Studies, Repairs and Maintence*, *1*(4), 580–592. https://doi.org/10.2495/HA-V1-N4-580-592

Martens, C., Nasser, H., Van Steen, C., Caspeele, R., & Verstrynge, E. (2022). The relation between concrete crack width and rebar corrosion level validated on a large set of experimental data. *Proceedings of fib Congress 2022*, 13–16 June 2022, Oslo, Norway, 2160–2169.

Meinen, N. E., & Steenbergen, R. (2018). Reliability levels obtained by Eurocode partial factor design - A discussion on current and future reliability levels. *Heron*, *63*(3), 243–301.

NEN 6700 TGB 1990 (2005). *NEN 6700: Technische grondslagen voor bouwconstructies - TGB 1990 - Algemene basiseisen*. NEN.

Nogueira, C. G., & Leonel, E. D. (2013). Probabilistic models applied to safety assessment of reinforced concrete structures subjected to chloride ingress. *Engineering Failure Analysis*, *31*, 76–89. https://doi.org/10.1016/j.engfailanal.2013.01.023

Nogueira, C. G., Yoshio, L., & Zacchei, E. (2023). Deterministic and probabilistic approaches for corrosion in RC structures: A direct proposed model to total service life predictions. *Case Studies in Construction Materials*, *18*, e01913. https://doi.org/10.1016/j.cscm.2023.e01913

Olsson, A., Sandberg, G., & Dahlblom, O. (2003). On Latin hypercube sampling for structural reliability analysis. *Structural Safety*, *25*(1), 47–68. https://doi.org/10.1016/S0167-4730(02)00039-5

Pandey, M., Viljoen, C., Way, A., Fischer, K., Sýkora, M., Diamantidis, D., Steenbergen, R. D. J. M., Lind, N., Frangopol, D. M., Yang, D. Y., Retief, J. V., André, J., Nathwani, J., & R. Lenner. (2024). Life safety in the reliability-based design and assessment of structures. *Structural Safety, 113*.

Parrott, L. J. (1990). Damage caused by carbonation of reinforced concrete. *Materials and Structures*, *23*(3), 230–234. https://doi.org/10.1007/BF02473023

Schueremans, L., & Van Gemert, D. (2004). Assessing the safety of existing structures: Reliability based assessment framework, examples and application. *Journal of Civil Engineering and Management*, *10*(2), 131–141. https://doi.org/10.1080/13923730.2004.9636297

Siemens, T., Polder, R., & de Vries, H. (1998). Design of concrete structures for durability. *Heron*, *43*(4), 227–244.

Steenbergen, R., & Vrouwenvelder, T. (2010). Safety philosophy for existing structures and partial factors for traffic loads on bridges. *Heron*, *55*(2), 123–139.

Steenbergen, R. D. J. M., Sýkora, M., Diamantidis, D., Holický, M., & Vrouwenvelder, T. (2015). Economic and human safety reliability levels for existing structures. *Structural Concrete*, *16*(3), 323–332. https://doi.org/10.1002/suco.201500022

Schiessl, P. (2006). *fib Bulletin 34 Model Code for service life design*. FIB.

Sykora, M. (2015). *Probabilistic reliability assessment of existing structures focused on industrial heritage buildings*. Czech Technical University in Prague.

Sykora, M., Diamantidis, D., Holicky, M., & Jung, K. (2017). Target reliability for existing structures considering economic and societal aspects. *Structure and Infrastructure Engineering*, *13*(1), 181–194. https://doi.org/10.1080/15732479.2016.1198394

Tanner, P., & Hingorani, R. (2015). Acceptable risks to persons associated with building structure. *Structural Concrete*, *16*(3), 314–322. https://doi.org/10.1002/suco.201500012

Trbojevic, V. M. (2009). Another look at risk and structural reliability criteria. *Structural Safety*, *31*(3), 245–250. https://doi.org/10.1016/j.strusafe.2008.06.019

Tuutti, K. (1982). *Corrosion of steel in concrete*. Swedish Cement and Concrete Research Institute.

Val, D. V., & Melchers, R. E. (1997). Reliability of deteriorating RC slab bridges. *Journal of Structural Engineering*, *123*(12), 1638–1644. https://doi.org/10.1061/(ASCE)0733-9445(1997)123:12(1638)

von Greve-Dierfeld, S., & Gehlen, C. (2016). Performance-based durability design, carbonation, part 3: PSF approach and a proposal for the revision of deemed-to-satisfy rules. *Structural Concrete*, *17*(5), 718–728. https://doi.org/10.1002/suco.201600085

Vořechovská, D., Teplý, B., & Chromá, M. (2010). Probabilistic assessment of concrete structure durability under reinforcement corrosion attack. *Journal of Performance of Constructed Facilities*, *24*(6), 571–579. https://doi.org/10.1061/(ASCE)CF.1943-5509.0000130

Vrijling, J. K., van Gelder, P. H. A. J. M., & Ouwenkerk, S. J. (2013). Criteria for acceptable risk in the Netherlands. In *Infrastructure risk management processes: Natural, accidental, and deliberate hazards* (pp. 143–157).

Vrouwenvelder, T., & Scholten, N. (2010). Assessment criteria for existing structures. *Structural Engineering International*, *20*(1), 62–65. https://doi.org/10.2749/101686610791555595

Vrouwenvelder, T., Scholten, N. P. M., & Steenbergen, R. (2011). *TNO-060-DTM-2011-03086 Veiligheidsbeoordeling bestaande bouw Achtergrondrapport bij NEN 8700*. TNO.

Yu, L., François, R., Dang, V. H., L'Hostis, V., & Gagné, R. (2015). Structural performance of RC beams damaged by natural corrosion under sustained loading in a chloride environment. *Engineering Structures*, *96*, 30–40. https://doi.org/10.1016/j.engstruct.2015.04.001

Yuan, Y., & Ji, Y. (2009). Modeling corroded section configuration of steel bar in concrete structure. *Construction and Building Materials*, *23*(6), 2461–2466. https://doi.org/10.1016/j.conbuildmat.2008.09.026

Zhao, Y., Zhang, X., Ding, H., & Jin, W. (2016). Non-uniform distribution of a corrosion layer at a steel/concrete interface described by a Gaussian model. *Corrosion Science*, *112*, 1–12. https://doi.org/10.1016/j.corsci.2016.06.021